https://doi.org/10.15407/ujpe71.6.536

SHEREN KHLAIF, MOHAMMAD ELSAID*, AYHAM SHAER

Department of Physics, Faculty of Science, An-Najah National University
*(Nablus, West Bank, Palestine; *e-mail: mkelsaid@najah.edu)*

IMPACT OF MAGNETIC AND EXCHANGE FIELDS ON THE THERMAL PROPERTIES OF SILICENE MONOLAYERS

In this study, we analyze the Dirac Hamiltonian describing an electron within a monolayer of silicene, a two-dimensional nanomaterial, under the influence of externally applied electric and magnetic fields. The Hamiltonian incorporates an exchange-field term arising from the proximity of a ferromagnetic material layer. The energy eigenvalue spectrum is derived as a function of relevant physical parameters through direct diagonalization of the Hamiltonian matrix. We systematically examine the dependence of the Landau level spectra on the magnetic field, electric field, and induced exchange field. Furthermore, the statistical average energy of silicene and graphene monolayers is explored as a function of magnetic field strength, electric field intensity, and temperature. Additionally, the impact of the exchange field on the statistical average energy of a silicene/ferromagnetic hybrid structure is investigated. The thermal properties, including heat capacity and entropy, are analyzed as functions of magnetic field, electric field, exchange field, and temperature for both silicene and graphene monolayers. This comprehensive analysis provides insights into the interplay between external fields, material-specific properties, and thermal behavior in these two-dimensional systems.

Keywords: silicene, 2D nanomaterials, exchange-field effect, thermal properties, heat capacity, entropy.

1. Introduction

Research on 2D monolayer materials has become a focal point in condensed matter physics [1–5]. Graphene, composed of carbon (C) atoms arranged in a honeycomb lattice [6], was the first experimentally realized 2D crystalline material. More recently, silicene, a single layer of silicon (Si) atoms forming a buckled honeycomb structure, has been successfully synthesized on metal surfaces [7–10].

Citation: Khlaif Sheren, Elsaid Mohammad, Shaer Ayham. Impact of magnetic and exchange fields on the thermal properties of silicene monolayers. *Ukr. J. Phys.* **71**, No. 6, 536 (2026). https://doi.org/10.15407/ujpe71.6.536.

Graphene monolayers exhibit ultra-high electron mobility at room temperature due to their zero-energy band gap, rendering electrons effectively massless. However, this property limits graphene's applicability in logic-based devices, as transistors with graphene channels cannot be fully switched off [5]. Silicene has garnered significant attention owing to its unique attributes: (1) The spin-orbit interaction (SOI) in silicene is substantially stronger than in graphene, resulting in a band gap of 3.9 MeV compared with graphene's 24 MeV [8]. (2) The buckled lattice structure of silicene introduces a potential difference between its two sublattices, enabling tunable electronic properties.

Various 2D nanostructures derived from group IV elements, such as silicene [11–12], phosphorene, germanene, and stanene, have been synthesized using di-

verse experimental techniques [14–17]. The buckling of Si atoms was first reported by Shiraishi and Takeda in 1994 [18], highlighting the ability to control the band structure of silicene and similar 2D materials through external electric fields, which modulate the band gap.

Investigating the magnetic and thermal properties of silicene and other 2D materials is a critical area of research in nanoscience. For instance, Tayyaba Aftab explored the behavior of a silicene monolayer under perpendicular electromagnetic fields and the influence of ferromagnetic materials [19]. Additionally, researchers have demonstrated that vertical electric fields can induce a band gap opening in semimetallic buckled silicene and germanene monolayers [20]. Elsaid *et al.* employed exact diagonalization and $1/N$ approximation methods to study the thermodynamic, magnetic, and electronic properties of silicene and related 2D materials [21–27].

In this study, we examine electrons confined within silicene and graphene 2D monolayers. The Hamiltonian matrix, incorporating perpendicular magnetic and electric fields as well as ferromagnetic interactions, is diagonalized to derive the energy expression as a function of physical parameters. The resulting eigenenergy serves as a fundamental input for calculating the partition function, which in turn enables the determination of thermal properties such as heat capacity and entropy.

2. Theory and Method of Calculations

The silicene layer is positioned in the x-y plane on top of a ferromagnetic material, subjected to both electric and magnetic fields. The external magnetic field is aligned along the growth direction, i.e., the z-axis, expressed as $\mathbf{B} = (0, 0, B)$. Due to the buckled lattice structure of silicene, a potential difference arises between its two sublattices, effectively generating an internal electric field perpendicular to the silicene layer. Consequently, the single-electron Hamiltonian for silicene in the presence of a perpendicular magnetic field, an electric field, and the influence of a ferromagnetic material can be written as:

$$H_D = \hbar v \left[\left(k_x + \frac{eA_x}{\hbar}\right)\tau_z\sigma_z + \left(k_y + \frac{eA_y}{\hbar}\right)\tau_z\sigma_z\right] - \\ - \Delta_{so}\left(\tau_z s_z \sigma_z\right) + \Delta_z\sigma_z + h s_z. \quad (1)$$

The first term in the Hamiltonian equation is the kinetic energy due to the applied magnetic field, eA is the potential momentum (momentum in the field) due to the interaction with a constant magnetic field acting on z-direction. $\mathbf{A}$ is the magnetic vector potential related to the external magnetic field $\mathbf{B} = \boldsymbol{\nabla} \times \mathbf{A}$. The vector potential in the Landau gauge is:

$$\mathbf{A} = (0, Bx, 0). \quad (2)$$

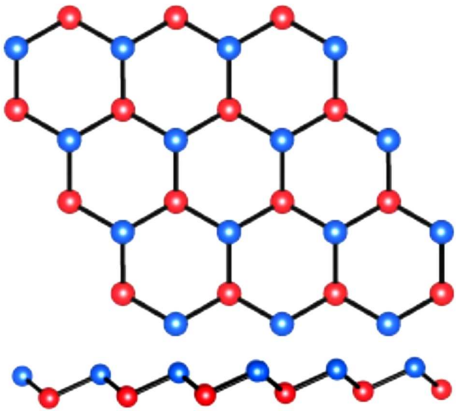

Fig. 1. Top: The crystal structure of silicene is based on the 2D honeycomb lattice. Due to the larger ionic size of silicon atoms, the silicene lattice is buckled with A and B sublattices located in vertically separated parallel planes. Bottom: Side view of the vertical buckling [7]

The second term in Eq. (1) is the spin–orbit coupling (SOC). Where Δso is the spin-orbital coupling gap, and taken to be 7.9 MeV [28]. The third term is the energy associated with electric field $\mathbf{E}$ with $\Delta_z = a_0 e\, E_z$, where E_z is an electric field applied perpendicular to the silicene layer, and $a_0 = 0.23$ Å is the buckling length.

The last term in Eq. (1) contains h which represents the exchange field effect due to the proximity, effect when silicene is placed on a ferromagnetic substrate, and is taken to be 9 MeV [29], $h = 1.1$ MeV [30]. The variation in values reflects different substrate–monolayer combinations (such as EuO) and varying strengths of exchange coupling reported in literature.

v is the Fermi velocity of the charge carrier (Dirac fermions), s_z is spin index, Δ_{so}: spin-orbital coupling gap. Δ_z is energy difference between Si atoms on A and B sites, unlike graphene, which is perfectly planar, silicene possesses a buckled honeycomb structure where the two sublattices (A and B) are vertically displaced by a distance $2l \approx 0.46$ Å as shown in Fig. 1. k_x, k_y is the momentum of charge carriers,

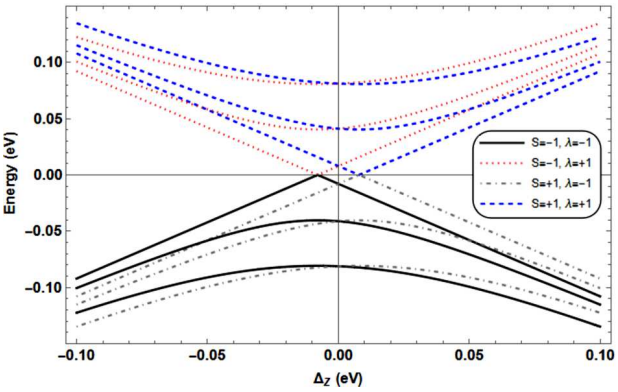

Fig. 2. Energy dispersion for K valley in silicene, as a function of a perpendicular electric field potential. For electrons, spin-up (dashed blue), spin-down (dotted red). For holes: spin-up (dot-dashed gray), spin-down (black). $\Delta_{so} = 7.9$ MeV, $B = 4.1T$, $h = 0$, $a_0 = 0.23$ Å, $n = 0$, 1, 2

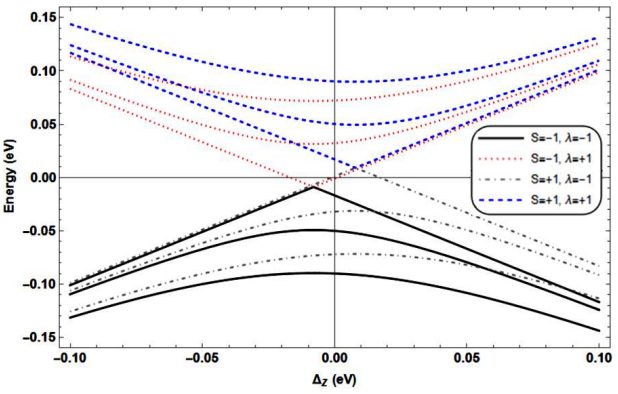

Fig. 3. Energy dispersion for K valley in silicene, as a function of a perpendicular electric field potential. $\Delta_{so} = 7.9$ MeV, $B = 4.1T$, $h = 9$ MeV, $a_0 = 0.23$ Å, $n = 0$, 1, 2. The color scheme is the same as in Fig. 2

A_x, A_y: vector potential components, σ_z: spin Pauli matrices, τ_z: ± 1, valley index.

By direct diagonalization of the Hamiltonian matrix, given in Eq. (1), we can obtain an expression for the energy spectrum for silicene as:

$$E(h, s_z, \lambda, n, \omega_l, \Delta_z, \tau_z) =$$

$$= h\, s_z + \lambda \sqrt{n(\hbar\omega_l)^2 + (\Delta_{so} s_z - \Delta_z \tau_z)^2}, \tag{3}$$

where $\lambda = +1, -1$ (electrons and holes), n is the Landau level index arising from the quantization of electronic orbits in a magnetic field, and $\omega_l = v\sqrt{\frac{2eB}{\hbar}} = = \frac{v}{l_B}$, where l_B is the magnetic length.

2.1. Statistical properties of silicene and other 2D nanomaterials

To derive the thermodynamic properties, such as heat capacity and entropy, for silicene and graphene, the partition function must be determined. We employ the well-known statistical relation for the partition function:

$$Z = \sum e^{-\beta E_n}, \tag{4}$$

$\beta = \frac{1}{k_B T}$, where k_B is the Boltzmann constant, T is the temperature, and E_n represents the energy eigenvalues of the system.

The partition function serves as the foundation for calculating thermodynamic quantities. Specifically, the average energy, entropy and heat capacity can be derived using the following relations, respectively:

$$\langle E \rangle = -\frac{\partial \ln Z}{\partial \beta}, \tag{5}$$

$$S = k_B \left(\ln Z - \beta \frac{\partial \ln Z}{\partial \beta} \right), \tag{6}$$

$$C_v = k_B \beta^2 \frac{\partial^2 \ln Z}{\partial \beta^2}. \tag{7}$$

These expressions allow us to analyze the thermal behavior of silicene and graphene under varying conditions, such as changes in temperature, magnetic field, and electric field (neglecting the phonon contribution to the thermal properties).

3. Results and Discussion

In this section, we will study the dependence of the energy spectrum of silicene and other 2D nanomaterials on the magnetic field strength, the energy difference between nanomaterial atoms on A and B sites (Δ_z) where $\Delta_z = a_0 e E_z$ and the exchange-field effect.

Figs 2 and 3 show the energy spectra for silicene as a function of the electric field energy in the presence of magnetic (B) field and exchange field for electrons and holes with spin-up and spin-down orientations. The plots display the variation of the energy spectrum of silicene with a perpendicular electric field potential for the states: $n =$ zero, 1, and 2. Energy level crossings in the spectral curves can be seen.

In the absence of an exchange energy ($h = 0$), the Dirac points in Fig. 2 are positioned very close to one another. However, when the exchange field energy is increased to 9 MeV, the dispersion relation

shows a shift in the Dirac points from zero to 0.01 eV, as illustrated in Fig. 3. This shift in the Dirac points becomes more pronounced as the exchange field is further enhanced. Notably, the Dirac point for spin-up (↑) states in both valleys shifts to the conduction band, while the spin-down (↓) states shift to the valence band. This behavior enables spin polarization, which is a critical feature for spintronics applications.

The exchange field, being coupled to spin, plays a pivotal role in spin-dependent devices. These findings regarding the energy spectrum are consistent with the results reported in Ref. [19].

In the absence of an electric field, the plot in Fig. 4 shows the energy-level spectrum as a function of the magnetic field. We notice that all $n \neq 0$ levels scale as $\sqrt{B}$. The plot shows that the energy of the electron in the silicene layer increases as the magnetic field increases for excited states ($n = 1, 2, 3, ...$). The magnetic field here lifts the degeneracy of each subband.

In Fig. 5, when the electric field is increased from zero to 0.435 V/Å ($\Delta_z = 100$ MeV), the dispersion relation reveals a shift in the Dirac point from zero to 200 MeV. Additionally, the energy spectrum increases with increasing magnetic field B, and each Landau level splits into two branches. This behavior is expected due to the introduction of a new confinement term caused by the magnetic field. These findings are consistent with the results reported in Ref. [7].

We have also plotted in Fig. 6 the statistical average energy for silicene as a function of temperature, at a constant electric field, where $\Delta_z = 9$ MeV in (a) and $\Delta_z = 30$ MeV in (b), for different magnetic fields ($B = 5$, 10, and $15T$).

The variation of the statistical average energy with temperature, considering the effects of the magnetic field B and the electric field, is illustrated in Figs. 6, a and 6, b. For a fixed magnetic field strength ($B = 5T$), the average energy is observed to increase with rising temperature. This behavior is attributed to the thermal energy ($E_{\text{th}} = k_{\text{B}}T$), which increases the electron energy as the temperature increases. The onset of this increase occurs at approximately 30 K in Fig. 6, a and at 10 K in Fig. 6, b, respectively.

The comparisons between Figs 6, a and b for constant values of temperature and magnetic field, for example: ($T = 150$ K, $B = 15T$) show that the average energy in (a) equals 1.4134 MeV, whereas in Fig. 6, b it equals 1.933 MeV. The result is that, as Δ_z increases the average energy increases.

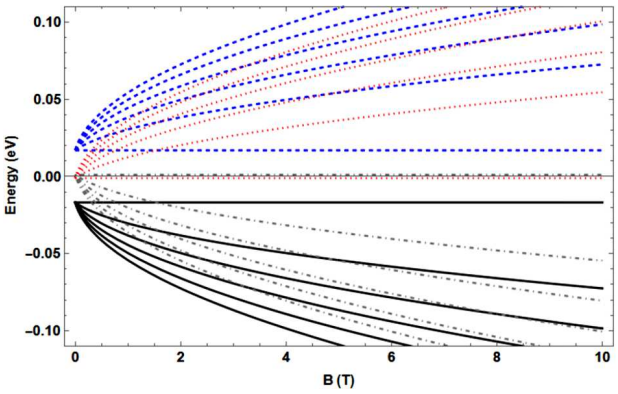

Fig. 4. Energy dispersion for K valley in silicene, varying with a perpendicular magnetic field. For electrons and holes. Δ_z = zero, $\Delta_{so} = 7.9$ MeV, $h = 9$ MeV, $\lambda = +1$ for electrons and –1 for holes n = zero, 1, 2, 3, 4, 5

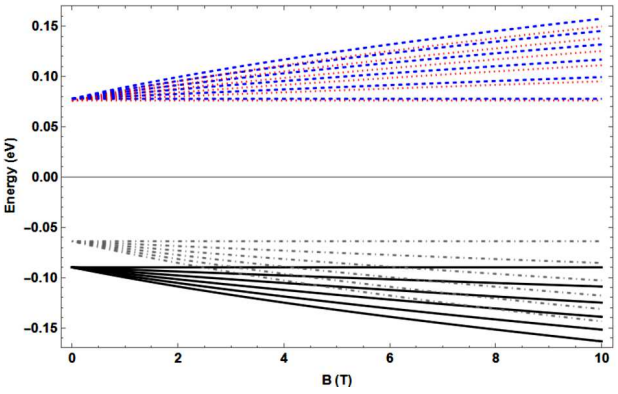

Fig. 5. Energy dispersion for K valley in silicene, varying with a perpendicular magnetic field. For electrons and holes. $\Delta_z = 100$ MeV, $\Delta_{so} = 7.9$ MeV, $h = 9$ MeV, $\lambda = +1$ for electrons and -1 for holes n = zero, 1, 2, 3, 4, 5

For graphene, we analyze the statistical average energy as a function of temperature, as depicted in Fig. 7 and find that the average energy similarly increases with rising temperature. However, it is observed that the rate of increase in average energy is more pronounced in silicene compared to graphene. This difference arises due to the presence of spin–orbit interaction (SOI) in silicene, with a strength of $\lambda_{so} = 3.9$ MeV, whereas in graphene it is effectively zero.

In Fig. 8, a, the dependence of the statistical average energy on the magnetic field is illustrated, incorporating the effects of both temperature and magnetic field. From Figs. 8, a and 8, b, it is evident that for a fixed magnetic field ($B = 5T$), the average en-

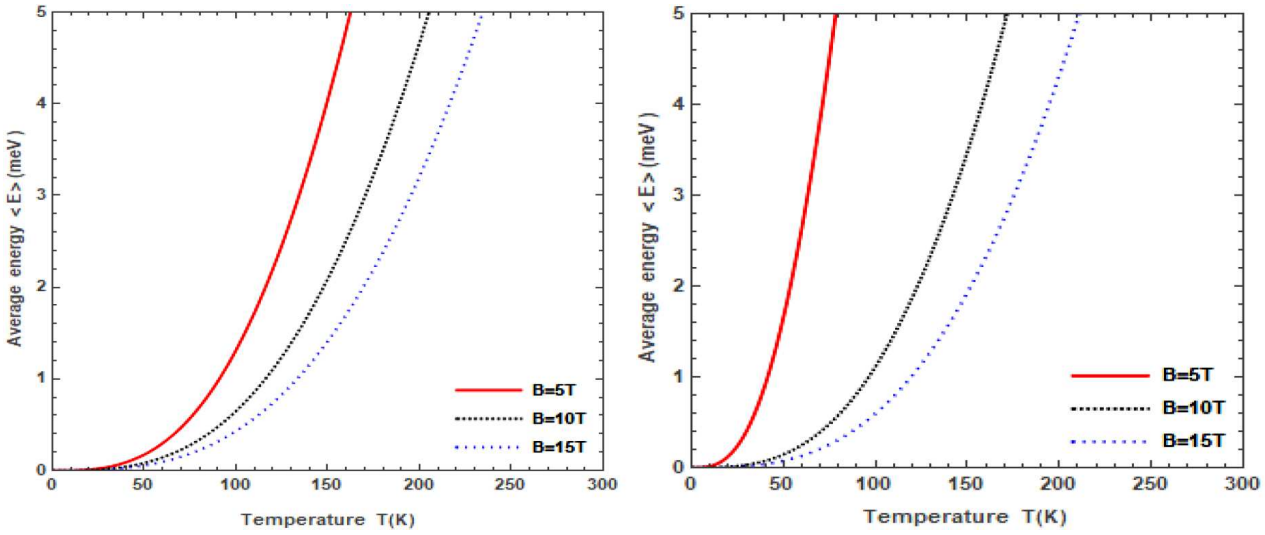

Fig. 6. Average energy for silicene as a function of temperature at different values of magnetic fields (B = 5, 10, and 15T) calculated at: Δ_z = 9 MeV (a), Δ_z = 30 MeV (b)

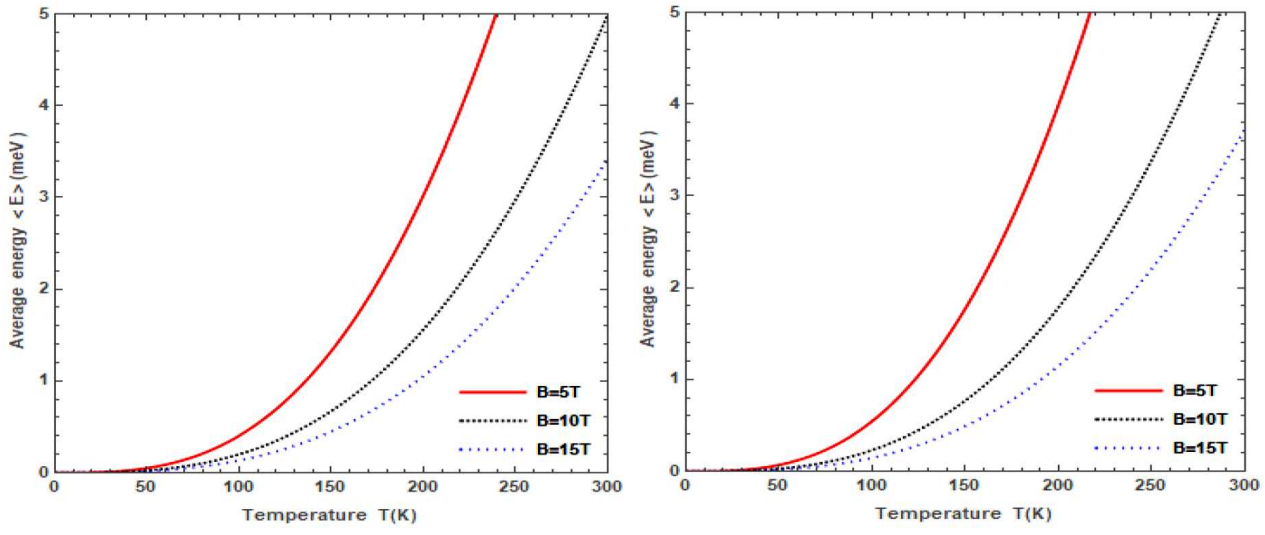

Fig. 7. Average energy for graphene varies with T (K) at different values of magnetic fields B = 5, 10, and 15T calculated at: Δ_z = 9 MeV (a), Δ_z = 30 MeV (b)

ergy increases as the temperature rises. This trend is attributed to the thermal energy, which elevates the electron energy and, as a result, leads to an increase in the statistical average energy.

Fig. 8, b, shows that as the exchange effect increases, the average energy curve decreases. The average energy is sensitive to the magnetic field only at low values of B.

Fig. 9 shows the heat capacity of silicene as a function of temperature (T) for different magnetic fields. It can be observed from Fig. 9 that at a fixed electric field, as T increases, the heat capacity increases, and it approaches an asymptotic constant value; $C_v \approx 2.2k_{\mathrm{B}}$ when T increases. In the absence of the energy difference ($\Delta_z = 0$), as the magnetic field increases, the heat capacity decreases, as shown in

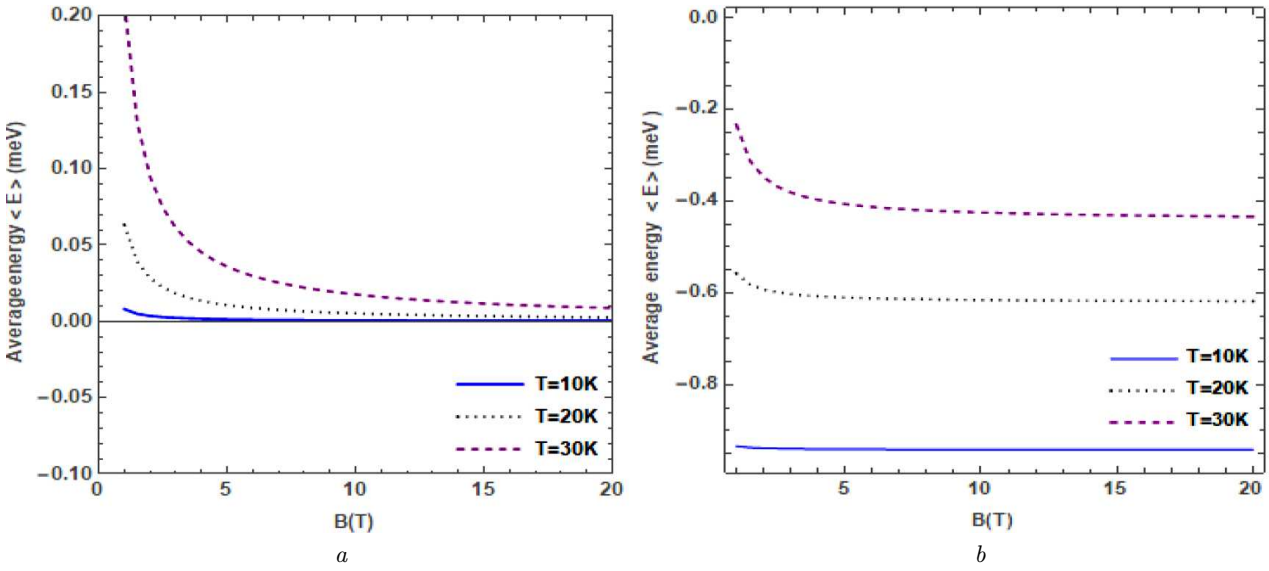

Fig. 8. Average energy for silicene varies with B at different values temperature calculated at: $\Delta_z = 5$ MeV, $h =$ zero (a), $h = 11$ MeV (b)

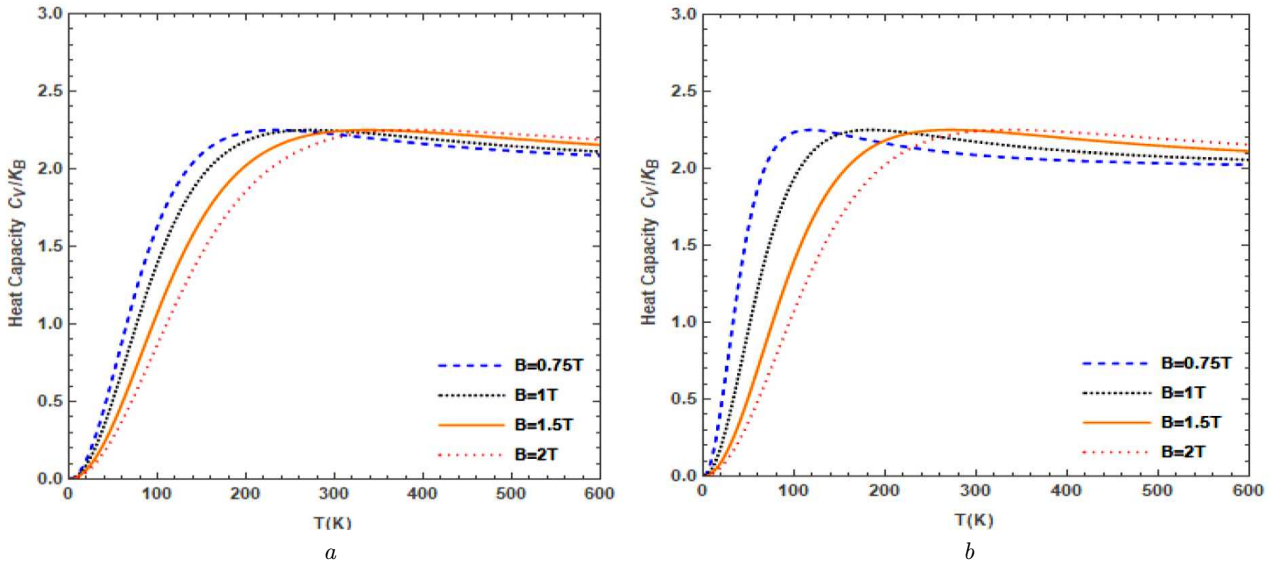

Fig. 9. For silicene, heat capacity per atom varying with temperature at different values of magnetic field $B = 0.75T$, $(B = 1T$, $B = 1.5T$, $B = 2T)$. $\Delta_z = 0$ MeV (a), $\Delta_z = 10$ MeV (b)

Fig. 9, *a*. However, if we increase the value of the energy difference, we note that the heat capacity curve exhibits a peak structure known as the Schottky effect. This means that when temperature increases, the heat capacity increases more rapidly in the first 150 Kelvin before approaching a constant asymptotic value of $2.2k_{\mathrm{B}}$.

Similar heat-capacity plots are shown for graphene in Fig. 10. The dependence of heat capacity on the magnetic field B is investigated for fixed temperatures as illustrated in Fig. 11 for silicene and Fig. 12 for graphene. At low magnetic field strengths, the heat capacity exhibits higher values, but as the magnetic field increases, the heat capacity decreases,

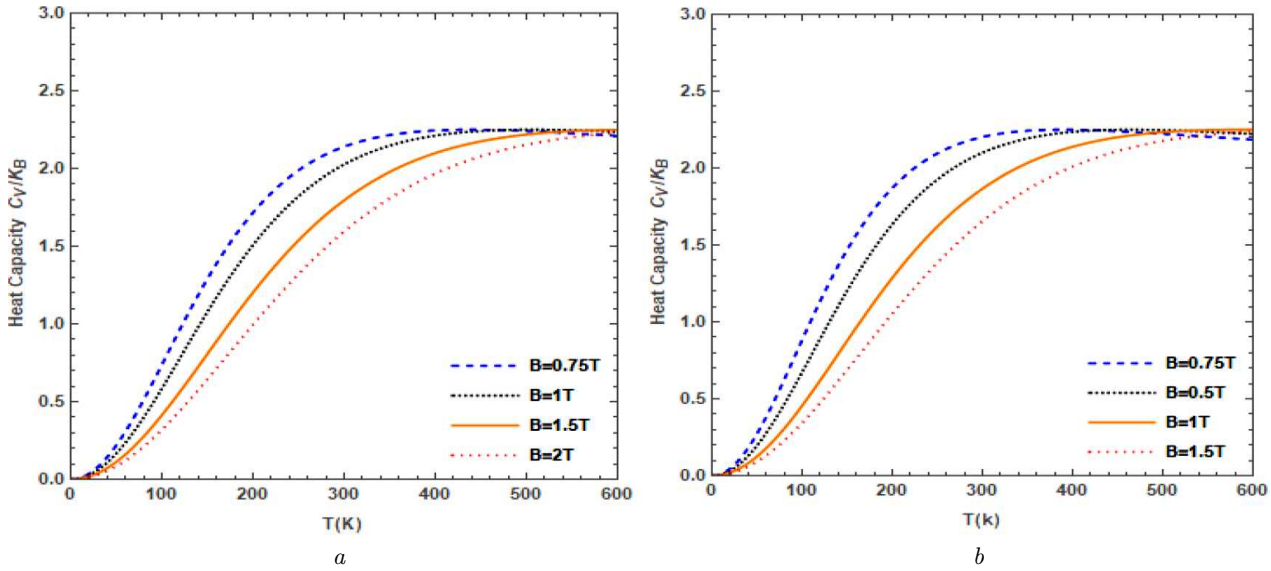

a *b*

Fig. 10. For graphene, heat capacity per atom varying with temperature at different values of magnetic field ($B = 0.75T$, $B = 1T$, $B = 1.5T$, $B = 2T$). $\Delta_z = 0$ MeV (*a*), $\Delta_z = 10$ MeV (*b*)

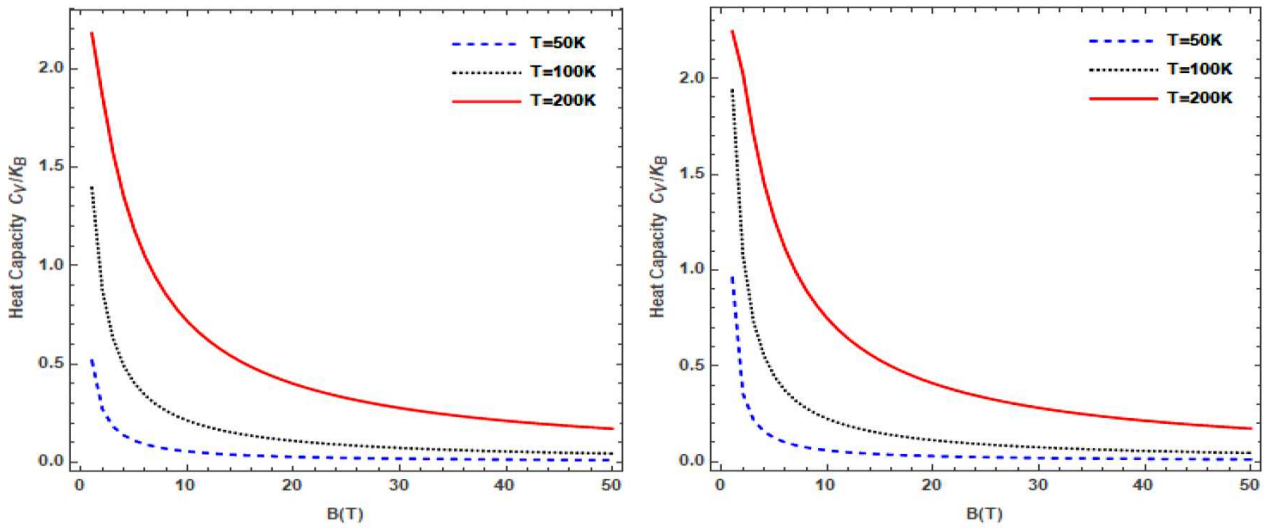

a *b*

Fig. 11. For silicene, heat capacity per atom varying with magnetic field at different temperatures $T = 50$ K, $T = 100$ K, $T = 200$ K at constant $\Delta_z = 0$ MeV (*a*), $\Delta_z = 10$ MeV (*b*)

eventually converging to a small constant value. This behavior arises because the available thermal energy (E_{th}) becomes insufficient to absorb heat or excite electrons to higher energy states under strong magnetic confinement within the 2D sheet. For instance, at $T = 50$ K, the thermal energy is minimal, causing the heat capacity to approach zero. Conversely, at higher temperatures, such as $T = 200$ K, the thermal energy increases significantly, leading to a heat capacity that approaches $2.2\,k_{\text{B}}$?

Fig. 13 shows the entropy of graphene as a function of temperature for different magnetic fields, with a constant energy difference. In the absence of Δ_z we find in Fig. 13, *a* that for the fixed value of B, as the temperature increases, the entropy of graphene also increases. This increase in entropy with tem-

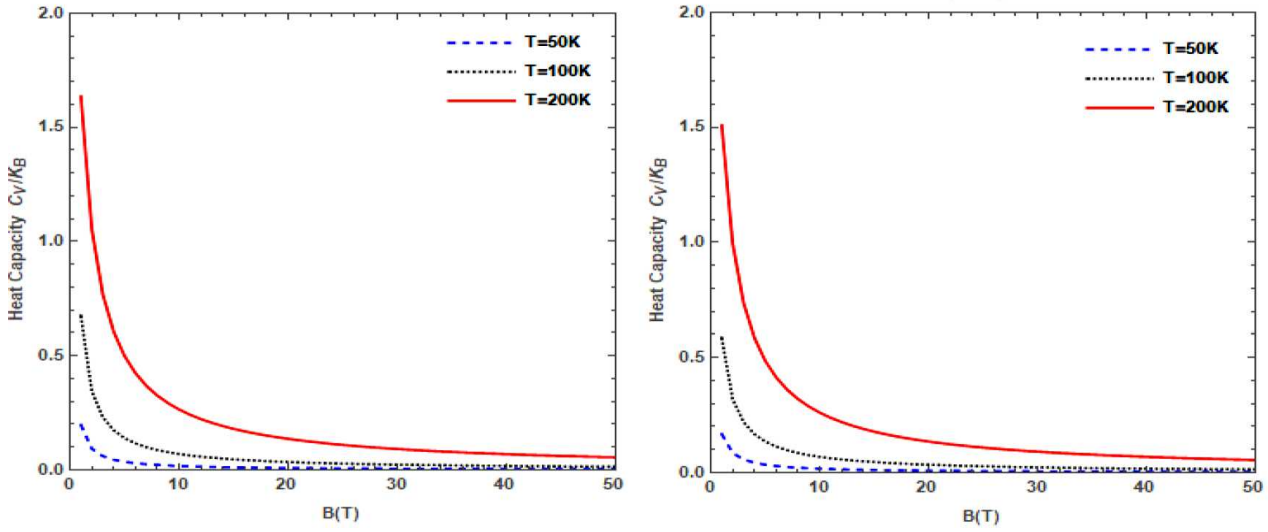

a *b*

Fig. 12. For graphene, heat capacity per atom varying with magnetic field at different temperatures $T = 50$ K, $T = 100$ K, $T = 200$ K at constant $\Delta_z = 0$ MeV (a), $\Delta_z = 10$ MeV

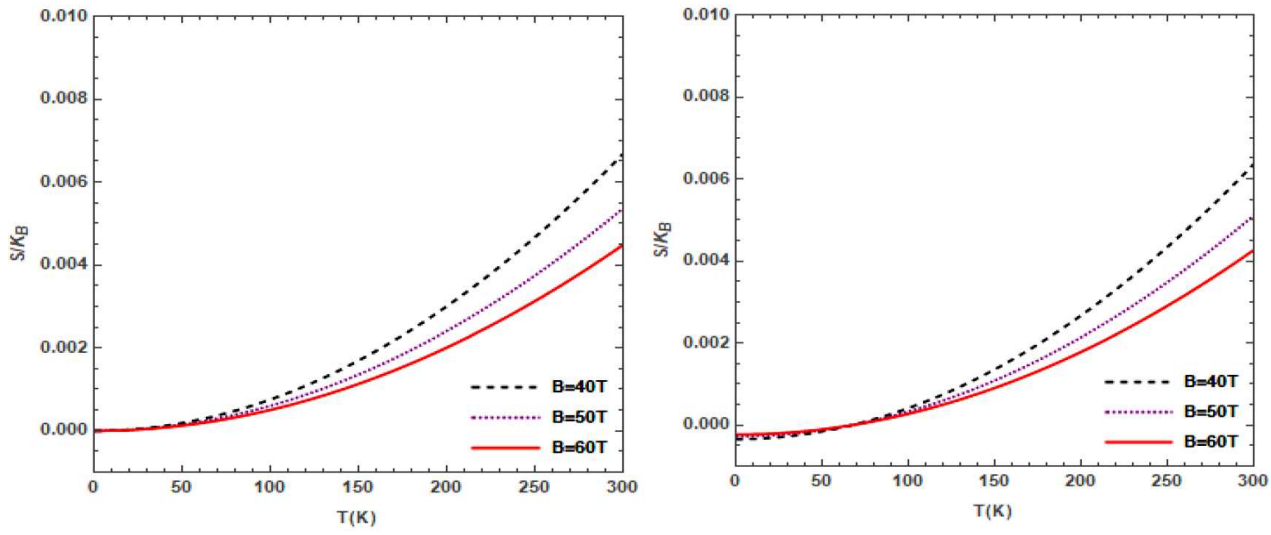

a *b*

Fig. 13. For graphene, entropy as a function of temperature at different values of magnetic fields $B = 40T$, $B = 50T$, $B = 60T$ at constant $\Delta_z = 0$ MeV (a), $\Delta_z = 10$ MeV (b)

perature is due to the enhancement of the thermal energy which increases the kinetic energy of electrons, which enhances the randomness of the system. From Fig. 13, it can be observed that the increase in entropy starts at $T \approx 50$ K. In Fig. 13, *a* and 13, *b*, the entropy decreases with increasing magnetic field, because the increase in the magnetic field restricts the movement of particles to Landau-type levels, so the turbulence and hence the entropy decreases.

In Fig. 14, we present the effect of the exchange field energy on the heat capacity of silicene as a function of temperature. The heat capacity is plotted for different values ($h = zero$, $h = 1$ MeV, $h = 1.5$ MeV, $h = 9$ MeV). For all values of the h parameter, the heat capacity C_v almost approaches zero as T

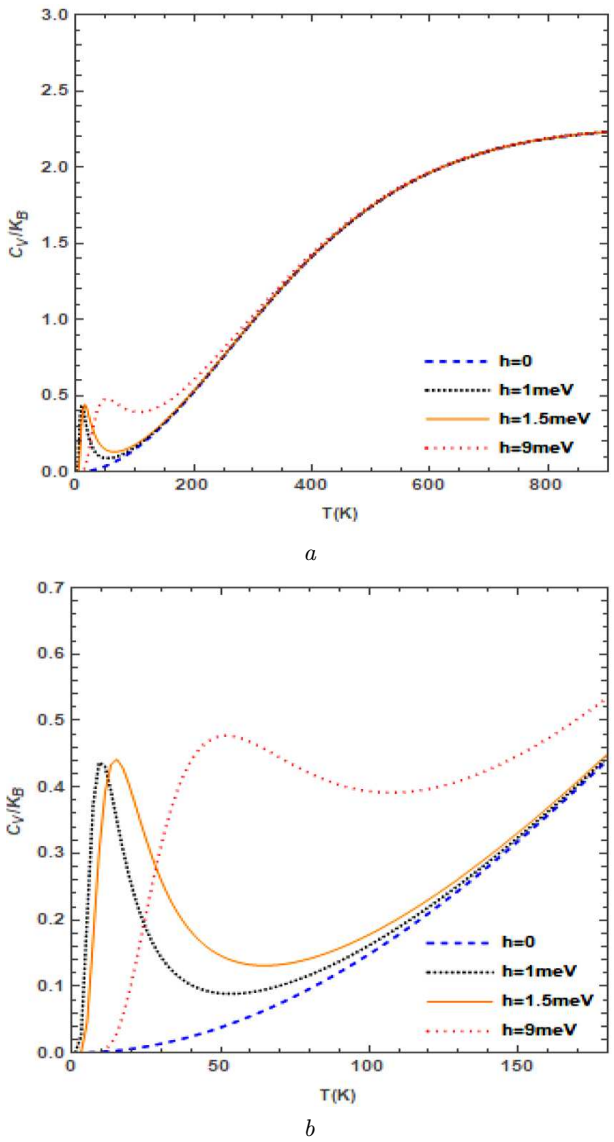

Fig. 14. For silicene, heat capacity per atom varying with temperature at different values of exchange-field parameter $h = 0$, $h = 1$ MeV, $h = 1.5$ MeV, $h = 9$ MeV at constant $\Delta_z = 10$ MeV, $B = 15T$. Large-scale temperature range (a). small-scale temperature range (b)

goes to zero. At zero temperature, when T increases from zero, C_v increases sharply and then decreases, exhibiting a peak-like structure. As temperature increases, the peak of heat capacity C_v shifts to a higher T and becomes broader.

As the exchange field energy increases, the number of crossings between states with the same orbital quantum number increases, thus, the density of states will increase too, then the probability of the heat absorption also increases. As temperature T increases further, the specific heat capacity becomes independent of the exchange effect and converges to a saturation value of $2k_{\mathrm{B}}$. We also noted that as the temperature keeps increasing, the heat capacity C_v tends to increase linearly because of an increase in thermal energy of electrons, which allows a greater number of states to be available for thermal excitation.

4. Conclusion

In this study, the Hamiltonian for a single electron in a silicene layer under the influence of electric and magnetic fields, along with the presence of a ferromagnetic material, was derived for silicene and graphene, both of which are 2D materials. The energy spectrum of electrons in these monolayers was obtained by solving the Hamiltonian using the direct diagonalization method.

In the initial phase of the study, the behavior of Landau levels (LLs) was examined as a function of the magnetic field, electric field, and exchange field for both the KK and K′K′ valleys, considering electrons and holes. This analysis was extended to various 2D materials, including silicene, graphene, stanene, and germanene.

The partition function, which characterizes the statistical properties of the system in thermodynamic equilibrium, is a crucial quantity for studying the thermal properties of 2D materials. An analytical expression was employed to compute the statistical average energy, taking into account various physical parameters. The results indicate that the electric field, magnetic field strength, and temperature significantly influence the statistical average energy. Specifically, the statistical average energy increases with the electric field but decreases with increasing magnetic field strength.

In the final part of the study, the effects of magnetic field strength, electric field, temperature, and exchange field on thermal quantities such as heat capacity and entropy were investigated. The heat capacity plot exhibits a small peak structure, known as the Schottky effect, which emerges as the electric field increases. Additionally, the heat capacity rises rapidly with temperature before approaching a constant asymptotic value, $C_v \approx 2.2\, k_{\mathrm{B}}$.

Furthermore, the behavior of entropy was analyzed, revealing that it increases with temperature as electrons gain kinetic energy from thermal energy. Conversely, entropy decreases with increasing magnetic field, electric field, and exchange field. These findings provide insights into the interplay between external fields, thermal energy, and the thermodynamic properties of 2D materials.

1. S. Bayda, M. Adeel, T. Tuccinardi, M. Cordani, F. Rizzolio. The history of nanoscience and nanotechnology: From chemical-physical applications to nanomedicine. *Molecules* **25**, 112 (2020).
2. V. Pokropivny, R. Lohmus, I. Hussainova, A. Pokropivny, S. Vlassov. *Introduction to Nanomaterials and Nanotechnology*, Vol. 1 (Tartu University Press, 2007).
3. M. Dendisová, A. Jeništová, A. Parchaňská, P. Matejka, V. Prokopec, M. Švecová. The use of infrared spectroscopic techniques to characterize nanomaterials and nanostructures: A review. *Anal. Chim. Acta* **1031**, 1 (2018).
4. J.F. Sierra *et al.* Room-temperature anisotropic in-plane spin dynamics in graphene induced by PdSe2 proximity. *Nat. Mater.* **24**, 876 (2025).
5. W. Gao, X. Shi, Y. Qiao, M. Yu, H. Yin. Strain-dependent near-zero and negative Poisson ratios in a two-dimensional $(CuI)P_4Se_4$ monolayer. *Phys. Rev. B* **109**, 075402 (2024).
6. R. Houça, A. Jellal. Thermodynamic properties of graphene in a magnetic field and Rashba coupling. *Phys. Scr.* **94**, 105707 (2019).
7. C.J. Tabert, E.J. Nicol. Magneto-optical conductivity of silicene and other buckled honeycomb lattices. *Phys. Rev. B – Cond. Matter and Mater. Phys.* **88**, 085434 (2013).
8. I. Ahmed, M. Tahir, K. Sabeeh. Electronic transport in silicene anti-dot lattices. arXiv:1402.6113 [cond-mat.mes-hall] (2014).
9. K. Mirabbaszadeh, M. Yarmohammadi, J. Khodadadi. Spin magnetic susceptibility of ferromagnetic silicene in the presence of Rashba spin-orbit coupling. *AIP Adv.* **7**, 035211 (2017).
10. F. Escudero, J.S. Ardenghi, P. Jasen. Magnetic oscillations in silicene. *J. Magn. Magn. Mater.* **454**, 131 (2018).
11. P. Vogt, P. de Padova, C. Quaresima, J. Ávila, E. Frantzeskakis, M.C. Asensio, A. Resta, B. Ealet, G. Le Lay. Silicene: Compelling experimental evidence for graphene-like two-dimensional silicon. *Phys. Rev. Lett.* **108**, 155501 (2012).
12. M. Tahir, K. Sabeeh, U. Schwingenschlögl. Quantum capacitance of an ultrathin topological insulator film in a magnetic field. *Sci. Rep.* **3**, 1075 (2013).
13. C. Cao, M. Wu, J. Jiang, H.P. Cheng. Transition metal adatom and dimer adsorbed on graphene: Induced magnetization and electronic structures. *Phys. Rev. B – Cond. Matter and Mater. Phys.* **81**, 205424 (2010).
14. L. Li, S.Z. Lu, J. Pan, Z. Qin, Y.Q. Wang, Y. Wang, G.Y. Cao, S. Du, H.J. Gao. Buckled germanene formation on Pt(111). *Adv. Mater.* **26**, 4820 (2014).
15. M.E. Dávila, L. Xian, S. Cahangirov, A. Rubio, G. Le Lay. Germanene: a novel two-dimensional germanium allotrope akin to graphene and silicene. *New J. Phys.* **16**, 95002 (2014).
16. F.F. Zhu, W.J. Chen, Y. Xu, C.L. Gao, D.D. Guan, C.H. Liu, D. Qian, S.C. Zhang, J.F. Jia. Epitaxial growth of two-dimensional stanene. *Nat. Mater.* **14**, 1020 (2015).
17. S. Jomehpour Zaveh, M.R. Rezaee Roknabadi, T. Morshedloo, M. Modarresi. Electronic and thermal properties of germanene and stanene by first-principles calculations. *Superlattices Microstruct.* **91**, 383 (2016).
18. K. Takeda, K. Shiraishi. Theoretical possibility of stage corrugation in Si and Ge analogs of graphite. *Phys. Rev. B* **50**, 14916 (1994).
19. T. Aftab. Valleytronics and phase transition in silicene. *Phys. Lett.* **381**, 935 (2017).
20. Z. Ni, Q. Liu, K. Tang, J. Zheng, J. Zhou, R. Qin, Z. Gao, D. Yu, J. Lü. Tunable bandgap in silicene and germanene. *Nano Lett.* **12**, 113 (2012).
21. A. Alhaj Ali, A. Shaer, M. Elsaid. Simultaneous effects of Rashba, magnetic field and impurity on the magnetization and magnetic susceptibility of a GaAs-semiconductor quantum ring. *J. Magn. Magn. Mater.* **556**, 169435 (2022).
22. M. K. Elsaid, M. Al-Nafaa, S. Zugail. The energy eigenvalues of the quantum dot helium using the shifted 1/N expansion method. *Dirasat, Pure Sci.* **36**, 1, (2009).
23. M. Elsaid, A. Shaer, E. Hjaz, M.H. Yahya. Impurity effects on the magnetization and magnetic susceptibility of an electron confined in a quantum ring under the presence of an external magnetic field. *Chinese J. Phys.* **64**, 9 (2020).
24. A. Shaer, M.K. Elsaid, M. Elhasan. The magnetic properties of a quantum dot in a magnetic field. *Turkish J. Phys.* **40**, 209 (2016).
25. M. Elsaid, E. Hijaz. Magnetic susceptibility of coupled double gaas quantum dot in magnetic fields. *Acta Phys. Pol. A* **131**, 1491 (2017).
26. F. Bzour, M. Elsaid, K.F. Ilaiwi. The effects of pressure and temperature on the energy levels of a parabolic two-electron quantum dot in a magnetic field. *J. King Saud Univ. Sci.* **30**, 83 (2018).
27. F. Bzour, M.K. Elsaid, A. Shaer. The effects of pressure and temperature on the magnetic susceptibility of semiconductor quantum dot in a magnetic field. *App. Phys. Res.* **9**, 77 (2017).
28. C.J. Tabert, E.J. Nicol. Valley-spin polarization in the magneto-optical response of silicene and other similar 2D crystals. *Phys. Rev. Lett.* **110**, 197402 (2013).
29. X.J. Qiu, Y.F. Cheng, Z.Z. Cao, J.M. Lei. Charge and efficient spin-valley polarization conductances in ferromagnetic silicene. *J. Phys. D: Appl. Phys.* **48**, 465105 (2015).

30. S.K. Wang, J. Wang. Spin and valley filter in strain engineered silicene. *Chinese Phys. B* **24**, 037202 (2015).

Received 12.02.25

Ш. Хлайф, М. Ельсаїд, А. Шаер

ВПЛИВ МАГНІТНИХ
ТА ОБМІННИХ ПОЛІВ НА ТЕПЛОВІ
ВЛАСТИВОСТІ МОНОШАРІВ СИЛІЦЕНУ

У дослідженні аналізується гамільтоніан Дірака, що описує електрон у моношарі силіцену, – двовимірному наноматеріалі, який перебуває під впливом зовнішнього електричного й магнітного полів. Гамільтоніан містить член, пов'язаний з ефектом обмінного поля, що виникає через близькість шару феромагнетного матеріалу. Спектр власної енергії отримано як функцію відповідних фізичних параметрів шляхом прямої діагоналізації матриці гамільтоніана. Систематично досліджено залежність спектрів рівнів Ландау від магнетного й електричного полів та індукованого обмінного поля. Крім того, досліджено середню статистичну енергію моношарів силіцену й графену як функцію напруженості магнетного й електричного полів і температури. Також досліджено вплив обмінного поля на середню статистичну енергію гібридної структури силіцен/феромагнетик. Теплові властивості, включно з теплоємністю й ентропією, аналізуються як функції магнетного й електричного полів, обмінного поля й температури – як для моношарів силіцену, так і для графену. Такий комплексний аналіз дає уявлення про вплив зовнішніх полів на характерні властивості матеріалу й теплову поведінку цих двовимірних систем.

Ключові слова: силіцен, 2D наноматеріали, ефект обмінного поля, теплові властивості, теплоємність, ентропія.